

# The Birth of a Cusp: The Unfolding of a ‘Boundary Catastrophe’

Robert S. Maier<sup>\*1</sup> and Daniel L. Stein<sup>†2</sup>

*Depts. of \*Mathematics and †Physics  
University of Arizona  
Tucson, AZ 85721, USA*

**Abstract.** We study a phenomenon, analogous to a phase transition, that takes place in the theory of noise-activated transitions between attractors. Large fluctuations away from any attractor tend to be concentrated along certain optimal trajectories, and the flow field of optimal trajectories may contain focal points, or cusps. Optimal trajectories may be viewed as Hamiltonian trajectories, and a cusp may be viewed as a cusp catastrophe in the Lagrangian manifold that the optimal trajectories trace out. As the parameters of a noise-driven system are changed, a cusp may emerge from a saddle point of the underlying deterministic dynamics. This corresponds to a cusp catastrophe being formed at the boundary of the Lagrangian manifold, and moving inward. It is possible to find a nonpolynomial normal form that unfolds the corresponding ‘boundary catastrophe’, in a space of higher dimensionality. Just as the quartic normal form for a cusp catastrophe resembles the scaling form for a classical (Ginzburg–Landau) phase transition, so the normal form for a boundary catastrophe resembles the scaling form for a nonclassical phase transition. Both have continuously varying exponents.

## I INTRODUCTION

Over the last few years, the *optimal trajectory* concept [1–3] has proved its usefulness in explaining the phenomenon of noise-driven transitions in bistable and multistable systems, and noise-driven fluctuations generally. Dynamical systems driven by weak noise wander only occasionally from the immediate vicinity of their attractors. In the limit of weak noise, in which fluctuations of any specified magnitude become exponentially rare, a fluctuation away from an attractor to the vicinity of any specified point is increasingly likely, in a relative sense, to occur along an optimal trajectory from the former to the latter. In an appropriate energetic sense, the optimal trajectory is a *path of least resistance*.

In what follows, we report preliminary results from a systematic investigation of the singular features that can appear in the flow field of optimal trajectories, in a two-dimensional noise-driven bistable system without detailed balance. In a sense that can be

---

<sup>1</sup>) Email: [rsm@math.arizona.edu](mailto:rsm@math.arizona.edu). Partially supported by US NSF grant PHY-9800979.

<sup>2</sup>) Email: [dls@physics.arizona.edu](mailto:dls@physics.arizona.edu). Partially supported by US NSF grant PHY-9800979.

made precise, optimal trajectories are analogous to the rays of geometrical optics. Optical rays in an inhomogeneous medium may focus, bounce off caustics, and cross one another. The same turns out to be true for optimal trajectories, if extended sufficiently far from an attractor [4–11].

The caustics and cusps that appear in geometrical optics, and also in the semiclassical limit of quantum mechanics [12], are examples of *generic catastrophes*, of the sort that have been studied in the mathematical field of catastrophe theory [13]. As such, they are fully understood, and have been classified. Any generic catastrophe has a polynomial ‘normal form’, and may be *unfolded* by an appropriate change of variables. However, the singular features in a flow field of optimal trajectories, even in a stochastic model with a two-dimensional state space, may be more complicated. In part, this is because in a stochastic system with more than a single attractor, the flow field typically does not extend over the entire state space, but has a natural boundary. As a parameter of the stochastic model is varied, a generic catastrophe (a cusp with two caustics emerging from it) may emerge from the boundary, and move inward. The phenomenon of emergence, which we term a *boundary catastrophe*, can be analysed in terms of a *non-polynomial* normal form.

We have pointed out elsewhere [8, 11] that singular features such as focal points (cusps) and caustics in the optimal trajectory flow field may have a significant effect on the rate of noise-driven transitions, especially when they coincide with the most probable path from one basin of attraction to another. The appearance of a boundary catastrophe, as a system parameter is varied, may accordingly affect the transition rate in a way reminiscent of a phase transition in condensed matter physics. The attendant critical phenomena include non-smoothness of the ‘action barrier’ (i.e., the effective energy barrier) that governs the exponential dependence of the transition rate on the noise strength, as the noise strength tends to zero. They also include a blowup of the pre-exponential factor (‘prefactor’) in the transition rate. Both phenomena are described by *critical exponents*. At a deeper level, the normal form for a boundary catastrophe resembles the scaling form for a nonclassical phase transition. Both have non-integer, continuously varying exponents.

## II PHENOMENOLOGY

The starting point for our analysis is a stochastic differential equation that models a noise-perturbed system with two state variables, namely

$$\dot{x}^i = u^i(\mathbf{x}) + \epsilon^{1/2} \eta^i(t), \quad \mathbf{x} \equiv (x^1, x^2). \quad (1)$$

The system dynamics in the absence of noise are specified by a ‘drift field’  $u^i = u^i(\mathbf{x})$ . The parameter  $\epsilon$  specifies the strength with which the noise  $\eta^i = \eta^i(t)$  couples additively to the state variables. We take the noise to be delta-correlated in time, i.e., to be white. That is,  $\langle \eta^i(t_1) \eta^j(t_2) \rangle = D^{ij}(\mathbf{x}) \delta(t_1 - t_2)$ . Here  $D^{ij}$  is a diffusion tensor, which in general may depend on  $\mathbf{x}$ .

Fig. 1

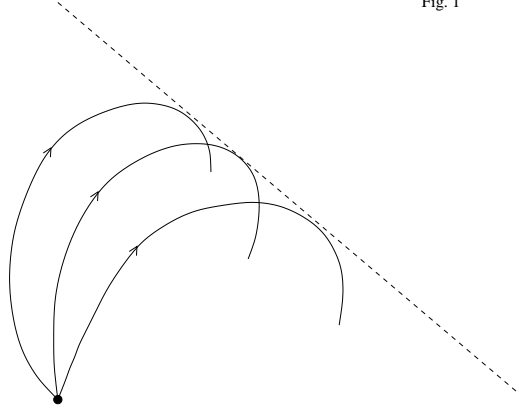


**FIGURE 1.** A sketch showing outgoing optimal trajectories bouncing off a caustic (indicated here by the dashed line).

This stochastic equation will serve to model the noise-perturbed dynamics of monostable, bistable, and multistable systems. These three alternatives are distinguished from one another by the pattern of attractors of the drift field  $\mathbf{u}$ . The simplest case is when the attractors are isolated points. If there is more than one attractor, each will be surrounded by a basin of attraction. The most commonly considered sort of noise-induced transition is a motion between adjacent basins, via a trajectory that passes through or near a saddle point on their common boundary. The case when the common boundary is an unstable limit cycle has also been considered [6, 14].

As noted, optimal trajectories show up in the weak-noise limit, i.e., in the  $\epsilon \rightarrow 0$  limit of solutions of the stochastic equation. Figure 1 shows the typical way in which singular features occur in a flow field of optimal trajectories. It shows a ‘fan’ or ‘pencil’ of trajectories emerging from a point attractor, and exhibiting singular behavior: even before they reach the boundary of the basin of attraction, the trajectories bounce off a singular curve (a caustic). The region beyond the caustic is ‘shadowed’ in the sense of geometrical optics. Normally, each point in a shadowed region is the endpoint of an optimal trajectory that takes a circuitous route.

The boundary catastrophe phenomenon is most easily visualized in symmetric models, i.e., models in which the drift field  $\mathbf{u}$  is symmetric through the  $x^1$  and  $x^2$  axes. An example would be [15]

$$u^1(x^1, x^2) = \lambda_1 x^1 (1 - (x^1)^2) - \alpha x^1 (x^2)^2 \quad (2)$$

$$u^2(x^1, x^2) = -|\lambda_2| x^2 \quad (3)$$

This is a model, parametrised by  $\alpha$ , in which there are point attractors at  $(x^1, x^2) = (\pm 1, 0)$ , whose basins of attraction are the right and left half-planes. The  $x^2$ -axis is the separatrix between the basins, and there is a saddle point at  $(0, 0)$ . The parameter  $\lambda_1 > 0$  measures the repulsion of the separatrix, and the parameter  $\lambda_2 < 0$  measures the extent to which fluctuations around the  $x^1$ -axis are suppressed. In the neighborhood of the saddle

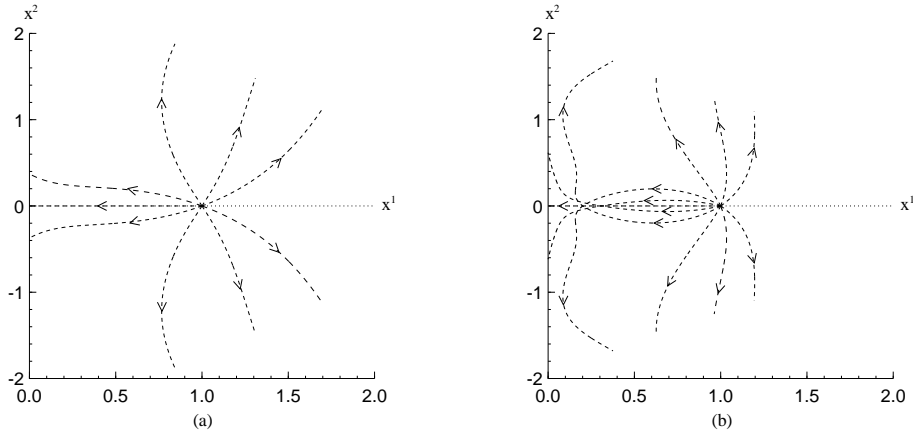


**FIGURE 2.** Sketches of the flow field of optimal trajectories emanating from the point attractor in the right half-plane. Part (a) corresponds to the pre-bifurcation case ( $0 \leq \alpha < \alpha_c$ ), and part (b) to the post-bifurcation case ( $\alpha > \alpha_c$ ), when there is a cusp on the positive  $x^1$ -axis.

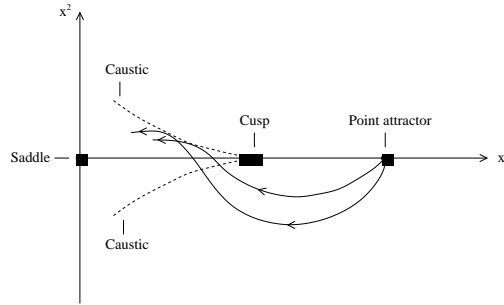


**FIGURE 3.** An exaggerated sketch of two of the optimal trajectories in Fig. 2(b), showing how they ‘bounce off’ a caustic. Both the caustic and the cusp from which it extends are indicated.

point, the deterministic dynamics of  $x^1$  and  $x^2$  decouple:  $\dot{x}^1 \approx \lambda_1 x^1$  and  $\dot{x}^2 \approx -|\lambda_2| x^2$ .

If  $\alpha = 0$  then  $\mathbf{u}$  is irrotational, i.e., is the negative gradient of a velocity potential. It is easy to verify that if the noise is isotropic and independent of state, e.g.,  $D^{ij}(\mathbf{x}) \equiv \delta^{ij}$ , then detailed balance holds, and the optimal trajectories are simply time-reversed integral curves of  $\mathbf{u}$ . Using now standard techniques [11], it can also be verified that if  $\alpha$  is increased from zero, up to a critical value  $\alpha_c$  the flow field of outgoing optimal trajectories of either point attractor (the point  $(1, 0)$ , say), resembles Fig. 2(a). Most of the other basin of attraction is in shadow, since the optimal trajectories are repelled by the saddle point, but there are no obvious singular features in the flow field. However, if  $\alpha$  is increased above  $\alpha_c$  the flow field resembles Fig. 2(b). A cusp emerges from the saddle point at  $(0, 0)$  and moves outward along on the  $x^1$ -axis. Two caustics extend from the cusp.

Figure 3 is an exaggerated drawing of the flow field when  $\alpha > \alpha_c$ , showing how the caustics extend from the cusp, and how the optimal trajectories bounce off the caustics.

Each point in the sharp-tipped region between the caustics, including the saddle point at  $(0, 0)$ , is the endpoint of *three* optimal trajectories. Usually, only one of them is the physical optimal trajectory terminating on the point: the other two have only a mathematical existence. However, points on the  $x^1$ -axis beyond the cusp, including the saddle point, are reached via two equally valid off-axis optimal trajectories. In the weak-noise limit, this means that exit from either half-plane is much more likely to go via either of two symmetrically placed off-axis noise-activated trajectories, than to go via the on-axis route. So at  $\alpha = \alpha_c$ , a *bifurcation* occurs. An examination of the  $\alpha$ -dependence of  $\mathbf{u}(x^1, x^2)$  shows that this is energetically plausible.

The weak-noise behavior of the inter-half-plane transition rate, precisely at  $\alpha = \alpha_c$ , is particularly interesting [11]. At any fixed  $\alpha$  other than  $\alpha_c$ , the mean passage time to the other half plane,  $\langle t_{\text{exit}} \rangle$ , behaves in the weak-noise ( $\epsilon \rightarrow 0$ ) limit as

$$\langle t_{\text{exit}} \rangle \sim C \exp(\Delta W/\epsilon) \quad (4)$$

This is a generalization of the usual Kramers formula [16]. Here  $\Delta W = (\Delta W)(\alpha)$  is the height of the effective energy barrier between the half-planes, and  $C = C(\alpha)$  is an appropriate pre-exponential factor.

Remarkably, as a function of  $\alpha$ , the effective energy barrier height  $\Delta W$  is non-smooth at  $\alpha = \alpha_c$ . In particular,  $(d^2/d\alpha^2)\Delta W$  at  $\alpha = \alpha_c^-$  and at  $\alpha = \alpha_c^+$  are unequal. The discontinuity in the second derivative arises because in the absence of detailed balance (i.e., the presence of non-conservative forces),  $\Delta W$  must be computed along the physical optimal trajectory extending to the saddle point, and that trajectory experiences a bifurcation at  $\alpha = \alpha_c$ . The singular behavior of  $\Delta W$  induces singular behavior of the prefactor:  $C$  passes through *zero* at  $\alpha = \alpha_c$ , i.e., the true weak-noise behavior of  $\langle t_{\text{exit}} \rangle$  at  $\alpha = \alpha_c$  contains a positive power of  $\epsilon$ . The singular behavior of both  $\Delta W$  and  $C$  can be captured by critical exponents [11].

### III ANALYSIS

A full understanding of the emergence of the cusp, at  $\alpha = \alpha_c$ , requires a detailed modeling of noise-activated behavior near the saddle point. Large noise-activated fluctuations are governed by a ‘quasipotential’ [6] function  $W(\mathbf{x})$  that specifies the size of the effective energy barrier between the attractor and any point  $\mathbf{x}$ . It turns out to be a classical action function for an auxiliary Hamiltonian dynamical system, with Hamiltonian

$$H(\mathbf{x}, \mathbf{p}) = \frac{1}{2} p_i D^{ij}(\mathbf{x}) p_j + u^i(\mathbf{x}) p_i. \quad (5)$$

The zero-energy trajectories of the Hamiltonian system are the optimal trajectories of the original system. They also generate  $W(\mathbf{x})$ :

$$W(\mathbf{x}) = \int_{\text{attractor}}^{\mathbf{x}} \mathbf{p}(\mathbf{x}') \cdot d\mathbf{x}' . \quad (6)$$

In the situation depicted in Fig. 3,  $W(\mathbf{x})$  is three-valued in the region between the caustics. That is because any point in this region can be reached by three optimal trajectories emanating from the point attractor; however, only the optimal trajectory with the least action is physical.

The analogy to a mean-field Ginzburg–Landau phase transition near the cusp can best be observed by Legendre-transforming  $W$ , replacing the variable  $x^2$  by the corresponding momentum variable  $p_2 = \partial W / \partial x^2$  [10, 11]. This yields

$$\widetilde{W}(x^1, p_2) = x^2 p_2 - W(x^1, x^2) \approx -c_2(x^1 - x_c^1)p_2^2/2 - c_4 p_2^4/4. \quad (7)$$

Here  $c_2$  and  $c_4$  are model-dependent constants, and  $x_c^1$  denotes the position of the cusp point on the  $x^1$ -axis. This change of variables is said to *unfold* the singularity, i.e., to remove the multiple-valuedness. The transformed action  $\widetilde{W}$ , as a function of  $x^1$  and  $p_2$ , is single-valued.

Geometrically, the three-valuedness of the action arises from a *fold* in the Lagrangian manifold in phase space. By definition, this manifold is traced out by the optimal trajectories emanating from the point attractor. As such, it is a two-dimensional submanifold of the full four-dimensional phase space parametrised by  $(x^1, x^2, p_1, p_2)$ , lying completely within the  $H = 0$  energy surface. Fig. 3 shows this fold projected down into the two-dimensional  $(x^1, x^2)$  subspace. The cusp and its associated caustics are generic catastrophes [13], and Eq. (7) is a *normal form* for the shape of a Lagrangian manifold near a cusp.

What happens at criticality, when  $\alpha = \alpha_c$ ? The manner in which the cusp is born depends on the parameter  $\mu \equiv |\lambda_2|/\lambda_1$ . Here we shall summarise our results on the ‘locally contractive’ (or ‘locally dissipative’) case  $\mu \geq 1$ . We defer the case  $\mu < 1$  (as well as a fuller treatment of  $\mu \geq 1$ ) to a separate paper.

When  $\alpha \leq \alpha_c$ , the most probable inter-half-plane transition path remains on the  $x^1$ -axis, and there is no cusp point on that axis. However, a careful numerical study shows that a *pair* of cusps, positioned symmetrically about the saddle point, is nonetheless present. These cusps were not apparent in Fig. 2(b). They are located on the boundary of the Lagrangian manifold, on or close to the  $x^2$ -axis. Figure 4 shows these cusps, and the optimal trajectories that bounce off their associated caustics. As  $\alpha \rightarrow \alpha_c^-$ , the cusps ‘neck down’ and approach the saddle point. At  $\alpha = \alpha_c$  they merge, forming a special *boundary catastrophe*. Once  $\alpha > \alpha_c$ , this turns into the familiar cusp catastrophe on the  $x^1$ -axis, which moves out towards the point attractor as  $\alpha$  increases further.

It is easy to check numerically that at criticality, i.e.,  $\alpha = \alpha_c$ , the cubic unfolding (7) is not appropriate. In Ref. [11] we presented a scaling theory to describe the behavior at  $\alpha_c$ . A nongeneric, nonpolynomial normal form was required.

For a full understanding of the boundary catastrophe phenomenon, a *joint unfolding*, describing the passage through criticality, is needed. Our work on the critical case has recently been expanded to a unified treatment that can account for behavior both on and off criticality, and both at and near the saddle point  $(0, 0)$ . This will be presented elsewhere [17]. Here we sketch a treatment in which much of the critical behavior can, surprisingly, be computed by a consideration of the linearised Hamiltonian dynamics

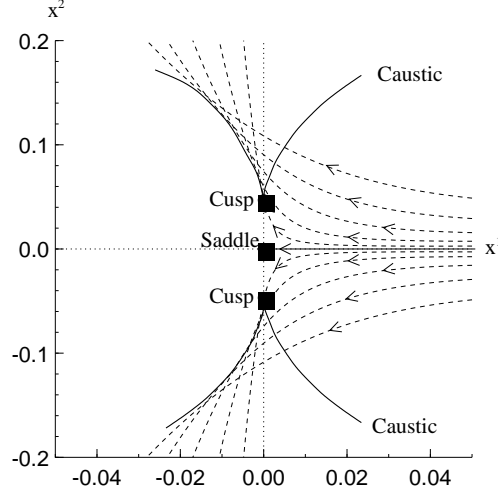


**FIGURE 4.** The flow field of trajectories just below criticality and with  $\mu > 1$ , showing the symmetric pair of cusps on the  $x^2$ -axis. As  $\alpha$  approaches  $\alpha_c$ , the cusps ‘neck down’ to the saddle point at  $(0, 0)$ , and at criticality they merge.

near  $(x^1, x^2; p_1, p_2) = (0, 0; 0, 0)$ . The presence of exponents that are non-mean-field-like, and vary continuously with  $\mu$ , will be clear.

A simple analysis (see also Ref. [18]) shows that in the vicinity of this point in phase space there are two stable directions,  $\mathbf{e}_s = (0, 1; 0, 0)$  and  $\tilde{\mathbf{e}}_s = (1, 0; -2, 0)$ , and two unstable directions,  $\mathbf{e}_u = (1, 0; 0, 0)$  and  $\tilde{\mathbf{e}}_u = (0, 1; 0, 2\mu)$ . The zero-momentum directions (no tilde) are eigendirections for deterministic trajectories, which follow the drift, and the others (denoted by a tilde) are eigendirections for optimal trajectories. In the linear approximation, any incoming optimal trajectory satisfies

$$(x^1, x^2, p_1, p_2) \approx C_s e^{-|\lambda_2|t} \mathbf{e}_s + \tilde{C}_s e^{-\lambda_1 t} \tilde{\mathbf{e}}_s + C_u e^{\lambda_1 t} \mathbf{e}_u + \tilde{C}_u e^{|\lambda_2|t} \tilde{\mathbf{e}}_u, \quad (8)$$

where the  $C$ ’s are constants (determined by the full Hamiltonian dynamics, but not needed explicitly).

We now index the ‘fan’ of optimal trajectories that approach the saddle point by a variable  $s$ , denoting (cf. Fig. 4) a given trajectory’s distance (at a fixed  $x^1$  near the saddle) from the  $x^1$ -axis (with  $s = 0$  corresponding to the on-axis trajectory). By symmetry considerations, each of the coefficients in (8) can be expanded in  $s$ , with  $C_s = a_1 s + \dots$ ,  $\tilde{C}_s = b_0 + b_1 s + \dots$ ,  $C_u = c_2 s^2 + c_4 s^4 + \dots$ , and  $\tilde{C}_u = d_1 s + d_3 s^3 + \dots$ . We can identify the passage through criticality with the vanishing, at  $\alpha = \alpha_c$  of  $c_2$  and  $d_1$ . So, setting  $\delta \equiv \alpha_c - \alpha$ , we take  $c_2$  and  $d_1$  as linearly proportional to  $\delta$ .

Eq. (8) comprises four scalar equations. Eliminating  $s$  and  $t$  among them, we can derive ‘equations of state’ relating  $\delta$  and the phase space variables. Near the  $x^1$ -axis, an approximate equation of state is found to be of the form

$$0 = (x^2 - p_2/2|\lambda_2|)^3 + k_1 \delta (x^1)^{2\mu} (x^2 - p_2/2|\lambda_2|) + k_0 (x^1)^{4\mu} p_2, \quad (9)$$

relating  $x^1$ ,  $x^2$ ,  $p_2$ , and  $\delta$ . The equation of state valid near the  $x^2$ -axis, i.e., the Lagrangian manifold boundary, relates  $x^1$ ,  $x^2$ ,  $p_1$ , and  $\delta$ , and is

$$0 = (x^1 + p_1/2\lambda_1)^3 + k'_1 \delta p_1^{2\mu-2} (x^2)^2 (x^1 + p_1/2\lambda_1) + k'_0 p_1^{4\mu-3} (x^2)^4. \quad (10)$$

A cusp is defined as the location where a momentum component first becomes multivalued as a function of  $\mathbf{x}$ . From Eq. (10), we find that (below criticality and for  $1 \leq \mu < 3/2$ ), the cusps neck down at rate governed by  $|x_{\text{cusp}}^2| \propto \delta^{3/2-\mu}$ . Similarly, Eq. (9) predicts that, above criticality and after the cusp emerges,  $x_{\text{cusp}}^1 \propto (-\delta)^{1/2\mu}$ . Both of these predictions have now been numerically confirmed.

This linearised Hamiltonian dynamics method can be extended to provide a unified treatment of both symmetric and nonsymmetric models, thereby unifying previous analyses both at criticality [11] and away from criticality [8, 10].

## REFERENCES

1. L. Onsager and S. Machlup, *Phys. Rev.* **91**, 1505 (1953).
2. M. I. Freidlin and A. D. Wentzell, *Random Perturbations of Dynamical Systems* (Springer-Verlag, New York/Berlin, 1984).
3. D. Ludwig, *SIAM Rev.* **17**, 605 (1975).
4. H. R. Jauslin, *Physica A* **144**, 179 (1987).
5. M. V. Day, *Stochastics* **20**, 121 (1987).
6. R. Graham, in *Theory of Continuous Fokker-Planck Systems*, edited by F. Moss and P. V. E. McClintock, volume 1 of *Noise in Nonlinear Dynamical Systems*, pp. 225–278 (Cambridge University Press, Cambridge, 1989).
7. R. S. Maier and D. L. Stein, *Phys. Rev. Lett.* **69**, 3691 (1992).
8. R. S. Maier and D. L. Stein, *Phys. Rev. Lett.* **71**, 1783 (1993).
9. V. A. Chinarov, M. I. Dykman, and V. N. Smelyanskiy, *Phys. Rev. E* **47**, 2448 (1993).
10. M. I. Dykman, M. M. Millonas, and V. N. Smelyanskiy, *Phys. Lett. A* **195**, 53 (1994).
11. R. S. Maier and D. L. Stein, *J. Stat. Phys.* **83**, 291 (1996).
12. L. S. Schulman, *Techniques and Applications of Path Integration* (Wiley, NY, 1981).
13. M. V. Berry, *Adv. Phys.* **25**, 1 (1976).
14. R. S. Maier and D. L. Stein, *Phys. Rev. Lett.* **77**, 4860 (1996).
15. This is a modified form of the drift field introduced in R. S. Maier and D. L. Stein, *Phys. Rev. E* **48**, 931 (1993), and studied in Ref. [11].
16. H. A. Kramers, *Physica* **7**, 284 (1940).
17. R.S. Maier and D.L. Stein, in preparation.
18. R.S. Maier and D.L. Stein, *SIAM J. Appl. Math.* **57**, 752 (1997).